

A High Accuracy Magnetostrictive Linear Position Sensor

Fernando Seco, José Miguel Martín, Antonio Ramón Jiménez and Leopoldo Calderón

Instituto de Automática Industrial, CSIC.
Ctra. de Campo Real, km 0,200, 28500 Arganda del Rey, Madrid, Spain
Corresponding e-mail: fseco@iai.csic.es
Webpage: <http://www.iai.csic.es/users/lopsi>

Published in *Sensors & Actuators A*, vol. 123–4, pp. 216-223 (sep. 2005)

Abstract

Magnetostrictive (MS) linear position sensors, which operate by measuring the time of flight of ultrasonic signals propagating in a waveguide, are one of the possible technologies for long range, absolute and high precision measurement. However, their accuracy is still far from the micrometer level achieved by standard differential sensors like optical encoders. This paper describes work in progress in a novel kind of MS linear position sensor, and considers the optimization of the processes of generation, transmission and reception of the ultrasonic waves in order to obtain higher precision. Preliminary results with the new sensor indicate a considerable improvement over the accuracy of standard MS sensors.

Keywords: Linear position measurement, magnetostrictive sensors ultrasonic propagation in waveguides.

1. Linear Position Sensors

Measurement of linear position is fundamental in many industrial processes, especially when used for feedback in computer numerical controls (CNC) for machine tool operation. The most common sensors, for a linear displacement of about 1 m, in order of increasing precision (and cost) are potentiometers, LVDTs, magnetostrictive, optical encoders and laser interferometers [1]. Their characteristics are summarized in table 1.

Besides these standard sensors, other alternative technologies in a research stage have been reported in the literature. A linear encoder based in the capacitive effect is described in [2], with non-linearity of $40\ \mu\text{m}$ (accuracy of $3\ \mu\text{m}$ after calibration) over a range of 150 mm. The PLCD sensor reported in [3] is based in the change of magnetic flux caused by the motion of a magnet along a soft magnetic core;

this sensor is similar in concept to an LVDT, but shows higher tolerance to changes in the separation of the cursor and the ruler. A similar idea, the variation of the inductance in a coil by saturation of a magnetic circuit is shown in [4]. Already existing sensors benefit also from the new magnetic materials like amorphous ribbons which are used as core elements. These materials provide superior linearity in LVDTs [5], therefore extending the measurement range of the device. They are also used as transmitting elements in displacement sensors based in magnetostrictive delay lines [6], obtaining high accuracy ($< 10\ \mu\text{m}$) over short ranges (20 mm).

Magnetostrictive (MS) linear position sensors constitute an interesting possibility as generic all-use sensors because they are by principle non-contact and absolute. These are very desirable characteristics for machine tool operation, as well as their non-optical nature which makes them resistant to typical contaminants of the machine tool environment like shavings and metalworking coolant fluid. However, in order to be competitive with linear encoders, their accuracy should be improved considerably. In this paper we will analyze the existing commercial MS linear position sensor and propose an improved version of it. Also we will show different aspects of its design, aimed at achieving high measurement precision. Finally we will report preliminary experimental results with a prototype of a position sensor and state some conclusions.

1.1. Magnetostrictive linear position sensors

In a MS sensor, the position is estimated from the time-of-flight (TOF) of ultrasonic signals generated in a waveguide at the mobile element by the magnetostrictive effect. The basic setup is shown in figure 1. The sensor consists in a ferromagnetic waveguide (usually a wire or a thin tube) that covers the

Sensor	Meas. range	Contact	Abs/Inc	Precision (μm)
LVDT	Small	No	Abs	250(*)
Potentiometric	Medium	Yes	Abs	400
Magnetostrictive	Large	No	Abs	200
Optical encoder	Large	No	Inc	5
Laser interferometer	Very large	No	Inc	0.1

Table 1: Characteristics of typical commercial linear position sensors: measurement range, contact between the cursor and the displacement axis, absolute/incremental nature and precision. The precision corresponds to a measuring range of 1000 mm, except for the LVDT(*), where it is 100 mm.

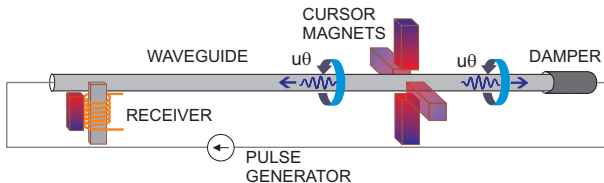


Figure 1: Conventional MS linear position sensor.

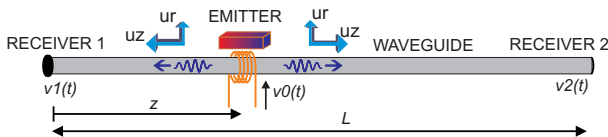


Figure 2: Principle of operation of the Micrus sensor.

measuring length, and a cursor formed by a set of magnets oriented perpendicularly to the tube, moving along the waveguide. Periodically a pulse generator sends an electric signal through the tube; the interaction of the magnetic field created by the current with that of the magnets creates a torsional stress in the waveguide which generates ultrasonic waves travelling in both directions. One of the waves is absorbed by a damper, while the other is picked by the receiver transducer. Measurement of the time of flight and knowledge of the propagation speed permits to estimate the cursor position z . The ultrasonic wave is generated by the Wiedemann effect [7] which is a twist of the waveguide produced by the interaction of the axial magnetic field with the current circulating through the waveguide. The stress in the metal couples to the torsional modes $T(0,m)$ of the waveguide, for which the displacement vector consists of only the azimuthal component (in cylindrical coordinates, $u = [0, u_\theta, 0]$ [8]). The ultrasonic pulse is converted back to an electrical signal through the inverse magnetostrictive (Villari) effect. The receiver transducer is a coil encircling a small tape of a magnetostrictive material placed next to one of the ends of the waveguide.

2. The Micrus sensor

The proposed MS linear position sensor, which is named Micrus, follows the working principle illustrated in figure 2. Although it resembles the conventional MS sensor, it presents the following innovative features:

- The position estimation is computed from the time delay between the ultrasonic signals received at both ends of the propagating tube.
- The Joule magnetostrictive effect is used to excite the longitudinal mode $L(0,1)$ of the waveguide, instead of the torsional mode $T(0,1)$.
- The piezoelectric effect is used for the ultrasonic signal reception instead of the inverse MS effect.

The next sections cover these characteristics in more detail.

2.1. Time Delay and Position Estimation

From figure 2, three signals are available for estimation of the cursor position in the Micrus sensor: the current in the generating coil, $v_0(t)$, and the ultrasonic signals received at the left and right piezoelectric transducers, $v_1(t)$ and $v_2(t)$. It is readily proved that a linear relationship holds between the cursor position z and any of three measurable time delays D_{ij} between signals $v_i(t)$ and $v_j(t)$.

We have found empirically that the most precise estimation of the position is obtained by use of the signals $v_1(t)$ and $v_2(t)$. Then, the position can be estimated as:

$$\hat{z} = \frac{1}{2}(L - c\hat{D}_{12}), \quad (1)$$

where L is the total length of the tube and c the propagation speed of the ultrasonic mode excited by the emitter, and \hat{z} is an estimation of the (actually unknown) measurand z .

From equation 1, the measurement of position reduces to a problem of precise time delay estimation (TDE), which, in our case, can be formulated as [9]:

$$\begin{aligned} v_1(t) &= s(t) + \eta_1(t) \\ v_2(t) &= s(t - D_{12}) + \eta_2(t), \end{aligned} \quad (2)$$

where $s(t)$ is the excitation signal in the cursor coil, and η_1 and η_2 are the respective contaminating noises, which we will assume to be Gaussian and uncorrelated to each other and the signals. In these conditions, it can be proved that the best estimation of the time delay \widehat{D}_{12} is yielded by the value that maximizes the correlation of signals:

$$\widehat{D}_{12} = \max \arg\{\widehat{R}_{12}(\tau) = \int v_1(t)v_2(t-\tau) dt\}. \quad (3)$$

The Cramér-Rao lower bound (CRLB) [10] sets a limit on the maximum accuracy which can be achieved in the estimation of the time delay from the set of equations 2. The standard deviation σ_D of the estimation of the delay \widehat{D} is:

$$\sigma_D^2 \geq \frac{1}{16\pi^2 BT f_0^2 \text{SNR}}, \quad (4)$$

a result which is applicable in the case of narrowband signals with central frequency f_0 , and spectra contained in the interval $|f| \in [f_0 - B, f_0 + B]$, where the bandwidth B is small with respect to f_0 . Likewise, the (linear) SNR must be high enough for unambiguous determination of the peak of the correlation $R_{12}(\tau)$ [11]. The observation time, T , is, in practice, equal to the duration of the signal $s(t)$.

Another important nuance for the TDE process is that we will actually work with sampled versions $v_1[n] = v_1(nt_s)$ and $v_2[n] = v_2(nt_s)$ of the signals in equation 2 (t_s is the sampling time). If we limit the precision in the estimation of the correlation peak to one sampling interval, the error committed can be as high as $\pm t_s/2$. For example, for a sampling frequency of $f_s = 2$ MHz, and taking $c \simeq 5$ $\mu\text{m}/\text{ns}$ in equation 1, the position error is bounded by $\sigma_z = 600$ μm , which is clearly too high for a MS sensor.

One method to estimate the time delay D_{12} with subsample precision consists in fitting an analytical curve to the three samples closest to the discrete maximum [12] (note that this requires a minimum sampling frequency $f_s > 6f_0$ in order to have at least three points in the positive semi-cycle of the correlation vector). The proper analytical curve to be fitted depends on the waveform $s(t)$ used for excitation of the ultrasonic signals. In the Micrus sensor we have employed a sine train modulated by a Hanning window:

$$s(t) = \frac{1}{2} \left[1 - \cos\left(\frac{2\pi t}{T}\right) \right] [S_H(t) - S_H(t-T)] \sin \omega_0 t, \quad (5)$$

where $S_H(t)$ is Heaviside's step function, $T = n_{\text{cyc}}/f_0$ is the total signal length, and n_{cyc} is the number of cycles of the signal. This waveform does

a good job in producing a finite duration signal with its energy contained in a small bandwidth.

For the signal of equation 5, the correlation takes a cosine shape near the peak; thus, an improved estimation of the delay is obtained by fitting the following function:

$$R[m] = a \cos(bm + c), \quad (6)$$

to the discrete maximum m_{max} and its neighboring points. The improved time delay is estimated as:

$$\widehat{D}_{\text{cos}} = (m_{\text{max}} - \frac{c}{b})t_s, \quad (7)$$

with:

$$\begin{aligned} \cos b &= \frac{\widehat{R}[m_{\text{max}} - 1] + \widehat{R}[m_{\text{max}} + 1]}{2\widehat{R}[m_{\text{max}}]} \\ \tan c &= \frac{\widehat{R}[m_{\text{max}} - 1] - \widehat{R}[m_{\text{max}} + 1]}{2\widehat{R}[m_{\text{max}}] \sin b}. \end{aligned} \quad (8)$$

2.2. Selection of the propagating mode

A waveguide with cylindrical symmetry can support three families of modes: torsional (denoted $T(0,m)$), longitudinal ($L(0,m)$) and flexural ($F(n,m)$) [8]. As the index n stands for the order of symmetry around the z axis, the torsional and longitudinal modes are axisymmetric ($n = 0$), while the flexural modes are asymmetric. The index m is used to order the propagating modes which can coexist in a family for a given operating frequency. In general, in any application which involves ultrasonic waves in solids, exploitation of a single propagating mode is recommended [13].

Ultrasonic signals travelling in a waveguide are subject to the phenomenon of dispersion, which is the variation of the phase and group speeds of the propagating waves with frequency. The theoretical dispersion curves in the low frequency range for the torsional, longitudinal and first two families of flexural modes are computed with the PCDISP software described in reference [14] and shown in figure 3.

It can be acknowledged from the figure that the mode $T(0,1)$ has the unique feature of being free from dispersive effects. This is one reason that leads to its use in the commercial MS sensors that we saw in section 1. In the Micrus sensor, however, we are interested in exploring the possibilities of using the faster propagating first longitudinal mode $L(0,1)$ for position measurement. With a new design of the emitter it is possible to obtain high transduction efficiency in the generation and reception processes, achieving the SNR required by equation 4 for accurate estimation of the time delay. For the $L(0,1)$ mode, the displacement vector has two nonzero entries $u = [u_r, 0, u_z]$;

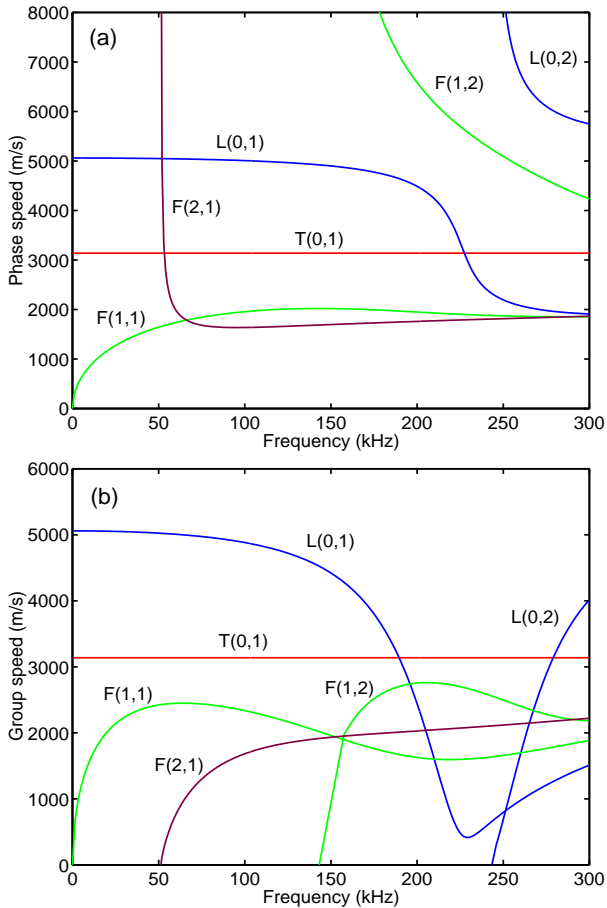


Figure 3: (a) Phase and (b) group speed curves for the torsional $T(0,m)$, longitudinal $L(0,m)$ and first two flexural modes, $F(1,m)$ and $F(2,m)$, existing in the frequency range 0-300 kHz, computed with PCDISP. The tube data is given in section 3.1.

however, at low frequencies, the radial component is much smaller than the axial one, $u_r \ll u_z$.

One consequence of choosing the mode $L(0,1)$ for operation of our sensor is that we need to quantify the effects of dispersion, unlike the case of the torsional mode. Because the frequency components of the signal travel at different phase speeds, the signal is distorted as it propagates along the waveguide. When those signals are used in the time delay and position estimation processes, the result is a systematic (i.e., position dependent) error in the measurement.

Several precautions can be taken to minimize the effects of dispersion. The width of the flat region of the $L(0,1)$ curve in figure 3 depends inversely on the thickness of the tube, so the thinnest available tube should be used. The excitation signal $s(t)$ should have a narrow spectral content, and the central frequency f_0 lie in a point where the dispersion curve is relatively flat ($dc_{ph}/d\omega \simeq 0$).

Where dispersion is unavoidable, theoretical or em-

pirical knowledge of the wavenumber-frequency relationship, $\xi(\omega)$, can be used to compensate the distortion suffered by the signal during the propagation in the waveguide. For example, Gorham and Wu [15] were able to restore the original shape of stress pulses caused by impact of steel spheres in pressure bars. Wilcox [16] has developed an optimized algorithm based on use of the FFT which could be employed for real time correction of dispersive effects.

To check if these methods are really needed, we performed simulations of the propagation of signals in the tube employed in the Micrus system, and the position estimation method of equation 1, for a total displacement range of 1 m. Using the software PCDISP and the method described in [17], we studied the influence of two design parameters of the waveform $s(t)$ of equation 5: the central frequency f_0 and the number of cycles n_{cyc} , on the position estimation. The results are shown in figure 4 (the physical data for the transmitting tube is given in section 3.1). As expected, the position error increases with frequency, as the dispersion curve of mode $L(0,1)$ in figure 3 gets steeper and closer to the cutting frequency of mode $L(0,2)$. The position error decreases with growing signal length (narrower spectral content), becoming lower than $1 \mu\text{m}$ for $n_{cyc} > 4$ cycles. This is very convenient, because it allows to use relatively short (temporal or spatial) excitation signals, and obtain a longer measuring range for a given tube size.

As a conclusion of the simulation process, active correction of the dispersion effects is not needed for operating frequencies below 100 kHz, unless the error due to other sources is inferior to $2 \mu\text{m}$.

2.3. Magnetostrictive Emitter

The emitter transducer of the Micrus system is designed to produce maximum coupling to the chosen ultrasonic mode (longitudinal $L(0,1)$). To this end the Joule magnetostrictive effect (in which the static and dynamic fields are arranged in the axial direction [7]) is used instead of the Wiedemann effect.

The emitter transducer, shown in figure 5, consists mainly of two elements. A set of four Alcomax III magnets provide a bias field which brings the part of the tube under the cursor to a known state in the magnetization curve, reducing hysteretic effects and increasing measurement repeatability. In the central region, an excitation coil (10 mm long, consisting of 60 turns of copper wire), creates the dynamic signal responsible of the MS generation. The total field is then given by $H(z) = H_0 + H_1 \exp j2\pi f_0 t$, with H_1 being about 10 times smaller in magnitude than H_0 , in order to reduce harmonics created by the nonlinear generation of ultrasound.

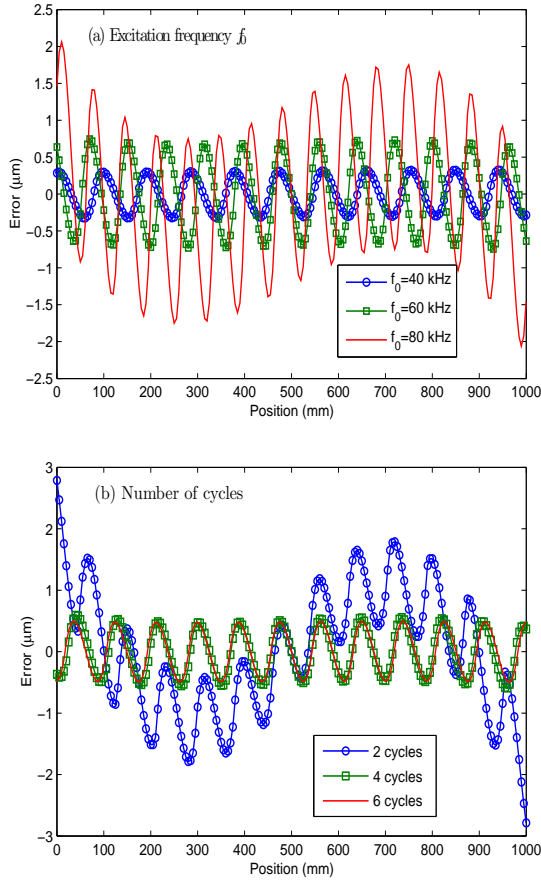


Figure 4: Simulation of the influence of (a) the central frequency f_0 (with $n_{cyc} = 6$); and (b) the number of cycles n_{cyc} (with $f_0 = 60$ kHz) of the excitation signal $s(t)$ on the systematic error in the position estimation.

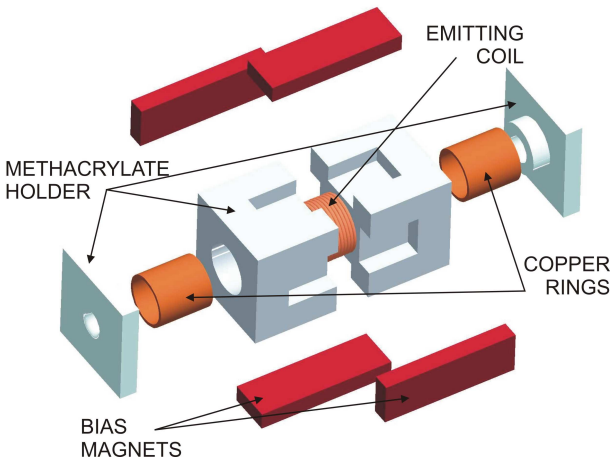


Figure 5: Magnetostrictive emitter of the Micrus sensor.

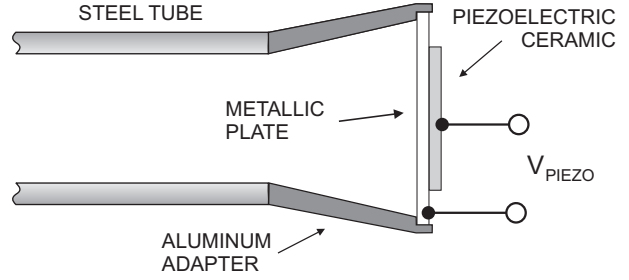


Figure 6: Arrangement of the piezoelectric receiver transducer at the end of the propagating tube.

Operation with the prototype showed that the position estimation process suffered from measurement hysteresis, caused in turn by the magnetic hysteresis of the metal of the transmitting element. A method was devised to compensate this problem, by focusing the dynamic magnetic field and choosing a convenient material (duplex stainless steel) for the propagating tube; more details of this procedure can be found in reference [18].

2.4. Piezoelectric receiver

We decided to use the piezoelectric effect instead of the inverse (Villari) magnetostrictive effect in order to enhance the sensitivity of the receivers and increase the SNR for the TDE process (as required by equation 4). Because there are no mobility requirements on the receiver transducers, they are simply stuck at the ends of the tube.

Excellent sensitivity to low frequency ($f_0 < 100$ kHz) ultrasonic waves in the tube was obtained with Murata MA40B8R piezoceramic disks. Each transducer was attached to the end of the tube with an aluminum adapter (see figure 6), which served to enhance the reproducibility of the measurements and obtain a higher correlation level between signals $v_1(t)$ and $v_2(t)$.

2.5. Selection of excitation frequency (f_0)

The experimental gain of the whole transducer system (comprising the processes of magnetostrictive generation, transmission in the waveguide and piezoelectric reception) is shown in figure 7. The response of the system is contained mainly in the 20-140 kHz range, achieving the maximum gain at 80 kHz, and with a second peak at a very low frequency (25 kHz). This second maximum corresponds to a resonance of the adapter piece.

Besides high gain, it is also desirable to obtain high correlation between the emitted and received signals, for optimal results of the correlation algorithm. An excitation frequency close to the maximum amplitude point (80 kHz) causes signal ringing and deteriorates the correlation value. Experimental waveforms

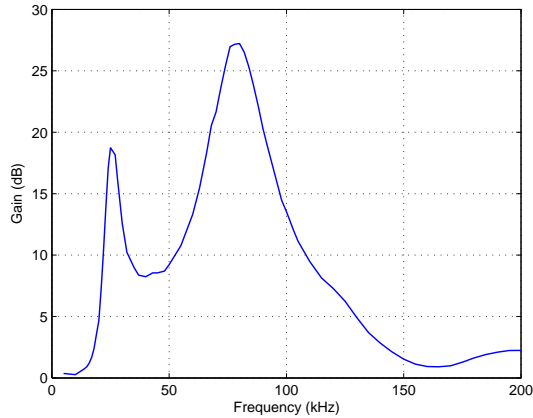


Figure 7: Experimental frequency response of the magnetostrictive-piezoelectric transduction process in the Micrus system.

for different values of the frequency f_0 along with the normalized correlation, are shown in figure 8, where the excitation waveform is given by equation 5 with $n_{cyc} = 8$.

With help of the data in this figure we finally selected the excitation frequency for Micrus as $f_0 = 60$ kHz. Lower frequencies, which empirically provide even higher correlation values, were avoided to keep the signal length down.

3. Empirical results

In this part we will describe the physical prototype in which we implemented the techniques of the last section and provide some experimental measurements obtained with the sensor.

3.1. Micrus prototype

The Micrus linear position sensor is shown in figure 9. The excitation signal (equation 5) is created in the central PC and transmitted via the GPIB bus to an arbitrary waveform generator (Agilent 33120A), filtered by an RC filter to smooth out the quantization steps of the 8-bit signal generator, amplified by a driver (ENI model 240L, with a gain of 50 dB) and put into the emitter coil. The current through this coil (signal $v_0(t)$ in figure 2) is measured with a 0.1Ω sensing resistance in series.

The transmitting waveguide is a stainless duplex steel tube (Sandvik SAF2304), with outer diameter 8 mm and thickness of 1 mm, and a total length of 1600 mm. The measurable range is 1000 mm, because a guard distance at both sides must be left to avoid interference of the emitted signals and the echoes from the extremes of the tube. This is known to be a limiting factor of the accuracy obtainable with magnetostrictive sensors [19]. The speed of

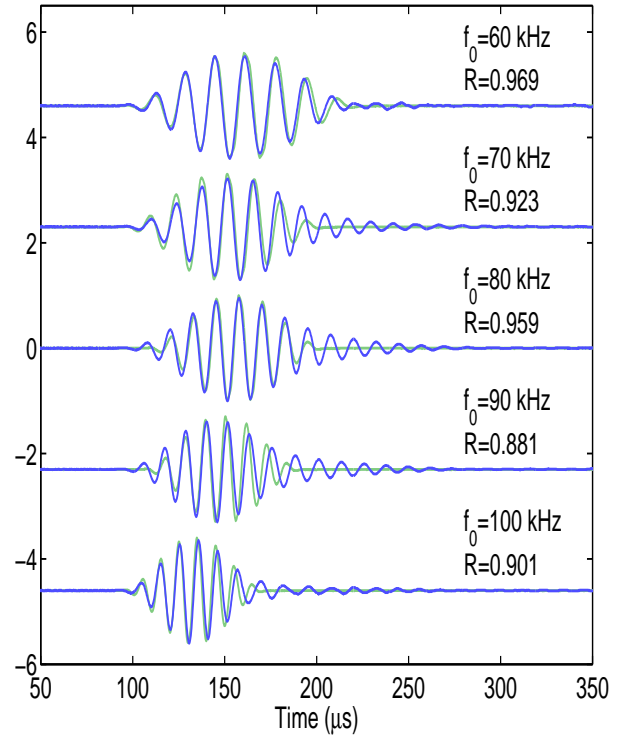


Figure 8: Emitted (light line) and received (dark line) signals for different excitation frequencies f_0 (signals have been normalized to unit amplitude), and values of their cross correlation.

sound of the L(0,1) mode at 60 kHz is very close to the bar velocity, $c_0 = 5060$ m/s. The tube is fixed to an optical bench (Newport X95-2), and held by silicon supports to avoid mechanical loading of the propagating ultrasonic waves. A commercial optical encoder (Fagor Automation model CX 1545, with range of 1.5 m and rated accuracy $\pm 5 \mu\text{m}$) is installed on the same frame for calibration and measurement of error purposes. The measurement is displayed in a digital readout and transmitted to the control PC through the serial port.

After reception of the propagating ultrasonic signals by the piezoceramics, they are amplified by instrumentation amplifiers, and isolated and decoupled with pulse transformers to achieve a high common mode rejection ratio. The three signals $v_0(t)$, $v_1(t)$ and $v_2(t)$ are simultaneously digitized with an acquisition card (Adlink PCI-9812), with a sampling frequency ranging between 1 and 5 MHz. The PC processes the acquired signals with an IIR Butterworth lowpass digital filter, with the cutoff frequency set at $2f_0$, in order to reject the out of band and quantization noise, and improve the SNR. The PC also runs the time delay and position estimation algorithms and provides a graphical interface and data analysis capabilities.

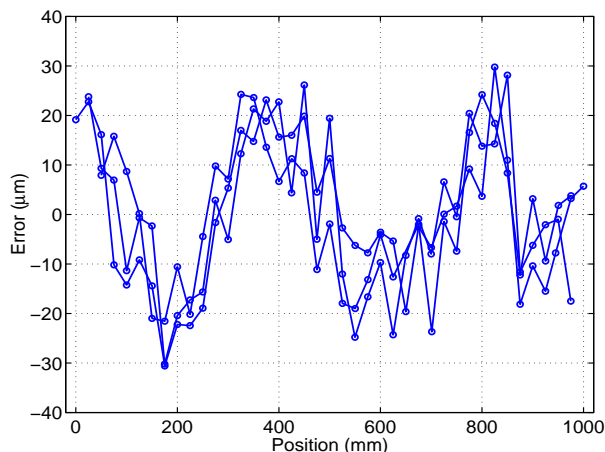


Figure 10: Typical error curve of the Micrus sensor, computed as the difference between the position estimation and the commercial optical encoder output. Three cycles over the whole measuring range are shown.

which match those of the machine tool in which they will be used. In magnetostrictive sensors, the most influential factor is rather the change of the propagation speed of the ultrasonic wave (in the order of $10^{-4} \text{ }^\circ\text{C}^{-1}$ for steel). In the laboratory experiment of figure 10, the temperature was kept constant at $25 \pm 0.25 \text{ }^\circ\text{C}$. For operation in realistic machine-tool environments, some method of active temperature compensation should be included (for example, integrating a temperature sensor in Micrus).

4. Conclusions

In this paper we have proposed a novel design of a magnetostrictive (MS) linear position sensor, which differs in several aspects from the existing sensors, and is intended to provide higher accuracy. The modifications include the measurement principle, the propagating mode selected and the receiver transducer.

The results with a prototype MS linear position sensor (Micrus) built according to those principles have shown an accuracy of $\pm 30 \text{ } \mu\text{m}$ over a 1 m range, significantly improving the performance of existing sensors.

We believe that the precision is ultimately limited by the mechanical and magnetic homogeneity of the tube which serves as the propagating element of the ultrasonic signals. The regularity of the obtained error pattern suggests that further improvements of the position sensor are possible and that the precision of MS linear position sensors may come closer to that of optical encoders.

References

- [1] J. G. Webster (Ed.), *The Measurement, Instrumentation and Sensors Handbook*, The Electrical Engineering Handbook Series, CRC Press, Springer and IEEE Press, 1999.
- [2] M. H. W. Bonse, F. Zhu, H. F. van Beek, A long-range capacitive displacement sensor having micrometre resolution, *Meas. Sci. Technol.* 4 (8) (1993) 801–807.
- [3] O. Erb, G. Hinz, N. Preusse, PLCD, a novel magnetic displacement sensor, *Sensors and Actuators A* 25-27 (1991) 277–282.
- [4] B. Legrand, Y. Dordet, J.-Y. Voyant, J.-P. Yonnet, Contactless position sensor using magnetic saturation, *Sensors and Actuators A* 106 (1-3) (2003) 149–154.
- [5] T. Meydan, G. W. Healey, Linear variable differential transformer (LVDT): linear displacement transducer utilizing ferromagnetic amorphous metallic glass ribbons, *Sensors and Actuators A* 32 (1992) 582–587.
- [6] V. Karagiannis, C. Manassis, D. Bargiotas, Position sensors based on the delay line principle, *Sensors and Actuators A* 106 (1-3) (2003) 183–186.
- [7] E. du Trémolet de Lacheisserie, *Magnetostriction: Theory and applications of magnetoelasticity*, CRC Press, 1993.
- [8] D. C. Gazis, Three-dimensional investigation of the propagation of waves in hollow circular cylinders. I. Analytical foundation. II. Numerical results., *J. Acoust. Soc. Am.* 31 (5) (1959) 568–578.
- [9] G. C. Carter, Coherence and time delay estimation, *Proceedings of the IEEE* 75 (2) (1987) 236–255.
- [10] J. Minkoff, *Signals, Noise and Active Sensors*, 1st Edition, Wiley Interscience, 1992.
- [11] A. Zeira, P. M. Schultheiss, Realizable lower bounds for time delay estimation: Part 2 - Threshold phenomena, *IEEE Trans. on Signal Processing* 42 (5) (1994) 1001–1007.
- [12] I. Céspedes, Y. Huang, J. Ophir, S. Spratt, Methods for estimation of subsample time delays of digitized echo signals, *Ultrasonic Imaging* 17 (2) (1995) 142–171.
- [13] J. L. Rose, *Ultrasonic Waves in Solid Media*, 1st Edition, Cambridge University Press, 1999.
- [14] F. Seco, J. M. Martín, A. R. Jiménez, J. L. Pons, L. Calderón, R. Ceres, PCDISP: a tool for the simulation of wave propagation in cylindrical waveguides, in: *9th International Congress on Sound and Vibration*, Orlando, Florida, USA, July 8-11, 2002, p. 23.
- [15] D. A. Gorham, X. J. Wu, An empirical method for correcting dispersion in pressure bar mea-

- surements of impact stress, *Meas. Sci. Technol.* 7 (9) (1996) 1227–1232.
- [16] P. D. Wilcox, A rapid signal processing technique to remove the effect of dispersion from guided wave signals, *IEEE Transactions on Ultrasonics, Ferroelectrics and Frequency Control* 50 (4) (2003) 419–427.
- [17] J. F. Doyle, *Wave Propagation in Structures*, 2nd Edition, Springer, 1997.
- [18] F. Seco, J. M. Martín, J. L. Pons, A. R. Jiménez, Hysteresis compensation in a magnetostrictive linear position sensor, *Sensors and Actuators A* 110 (1-3) (2004) 247–253.
- [19] A. Affanni, A. Guerra, L. Dallagiovanna, G. Chiorboli, Design and characterization of magnetostrictive linear displacement sensors, in: *Instrumentation and Measurement Technology Conference, IMTC 2004, Como, Italy, May 18-20, 2004*, pp. 206–209.